WIND ENERGY
Wind Energ. 2008; **11**:29–43
Published online 3 October 2007 in Wiley Interscience
(www.interscience.wiley.com) DOI: 10.1002/we.246

Research Article

Modelling of Power Fluctuations from Large Offshore Wind Farms

Poul Sørensen and Nicolaos Antonio Cutululis, Risø National Laboratory, Denmark
Antonio Vigueras-Rodríguez, Universidad Politécnica de Cartagena, Spain
Henrik Madsen and Pierre Pinson, Technical University of Denmark
Leo E. Jensen, Jesper Hjerrild and Martin Donovan, Dong Energy, Denmark

Key words:
admittance function;
equivalent wind speed;
power fluctuations;
wind farms

This paper deals with modelling of power fluctuations from large wind farms. The modelling is supported and validated using wind speed and power measurements from the two large offshore wind farms in Denmark. The time scale in focus is from 1 min to a couple of hours, where significant power fluctuations have been observed from these wind farms. Power and wind speed are measured with 1 s sampling time in all individual wind turbines in almost 1 year, which provides a substantial database for the analyses. The paper deals with diversified models representing each wind turbine individually and with aggregation of a wind farm to be represented by a single large wind turbine model. Copyright © 2007 John Wiley & Sons, Ltd.

Received 15 November 2006; Revised 4 June 2007; Accepted 2 August 2007

Nomenclature

α_{LF}	Parameter in $S_{LF}(f)$
β_{LF}	Parameter in $S_{LF}(f)$
$\gamma_{IEC}(f)$	Coherence functions in rotor plane as specified in IEC 61400-1
$\boldsymbol{\gamma}_{[r,c]}(f)$	Coherence functions between wind speeds at turbine r and turbine c
$\boldsymbol{N}(f)$	N element vertical vector of complex unity noise elements
σ	Standard deviation of the wind speed in a 10 minutes interval
σ_{am}	Standard deviation of wind speed in the ambient flow
σ_{wf}	Standard deviation of wind speed inside wind farm
$\tau_{[r,c]}$	Time it takes a wave to travel from wind turbine r to wind turbine c
C_T	Wind turbine thrust coefficient
A	Coherence decay factor used for coherence in wind turbine rotor plane
A_{lat}	Decay factor in $\boldsymbol{\gamma}_{[r,c]}(f)$ when the flow is lateral
A_{long}	Decay factor in $\boldsymbol{\gamma}_{[r,c]}(f)$ when the flow is longitudinal
$A_{[r,c]}$	Decay factor in $\boldsymbol{\gamma}_{[r,c]}(f)$
$d_{[r,c]}$	Distance between wind turbine r to wind turbine c
$F_{wt}(f)$	Wind turbine admittance function
Δf	Frequency increment in discrete PSDs
f	Frequency
f_0	Frequency parameter in $F_{wt}(f)$
f_1	Frequency parameter in $F_{wt}(f)$

*Correspondence to: Poul Sørensen, Risoe National Laboratory, Wind Energy Department, VEA-118, PO Box 49, DK-4000 Roskilde, Denmark.
E-mail: poul.e.soerensen@risoe.dk

$F_{wt}(f)$ Wind turbine admittance function
$F_{wf}(f)$ Wind farm admittance function
L_1 Length scale of turbulence, defined in IEC 61400-1
N Number of wind turbines in the wind farm
$P_{wf}(f)$ Produced electrical power of wind farm
$P_{wt[i]}(t)$ Produced electrical power of wind turbine i.
R Radius of wind turbine rotor
s_1 Separation (in rotor diameters) between wind turbine rows in wind farm
s_2 Separation (in rotor diameters) between wind turbine columns in wind farm
$S_{IEC}(f)$ Kaimal type PSD of wind speed used in IEC 61400-1
$\mathrm{S}(f)$ $N \times N$ wind speed cross power spectral density (CPSD) matrix
$S_{LF}(f)$ PSD for low frequencies
$S_{[rc]}(f)$ Element in $\mathbf{S}(f)$
$S_{u[i]}(f)$ PSD of the wind speed in a fixed point in the hub height of wind turbine i
$S_{u_{eq}[i]}(f)$ PSD of an equivalent wind speed $u_{eq[i]}(t)$ of wind turbine i
$u_{ave}(t)$ Average equivalent wind speed of all wind turbines in the wind farm
$u_{[i]}(t)$ Hub height wind speed of wind turbine i
$u_{eq[i]}(t)$ Equivalent wind speed of wind turbine i, which includes the smoothing of the wind speed due to the weighted averaging over the rotor
$U(f)$ Fourier transform of $u(t)$
$\mathbf{U}_{LT}(f)$ deterministic, lower triangular $N \times N$ matrix
x^* Complex conjugated of x
$\boldsymbol{x}^T$ Transposed of vector or matrix $\boldsymbol{x}$
V_0 Average wind speed in a 10 minutes interval
z Height above ground

Introduction

A major issue in the control and stability of electric power systems is to maintain the balance between generated and consumed power. Because of the fluctuating nature of wind speeds, the increasing use of wind turbines for power generation has caused more focus on the fluctuations in the power production of the wind turbines, especially when the wind turbines are concentrated geographically in large wind farms.

An example of this is observations of the Danish Transmission System Operator, Energinet.dk. According to Akhmatov *et al.*,[1] Energinet.dk has observed that power fluctuations from the 160 MW offshore wind farm Horns Rev in West Denmark introduce several challenges to reliable operation of the power system in West Denmark, and also that it contributes to deviations from the planned power exchange with the power system of Union for the Co-ordination of Transmission of Electricity (UCTE). It has also been observed that the time scale of the power fluctuations is from tens of minutes to several hours.

This paper presents two models for simulation of power fluctuations from a wind farm. The first model is a diversified model, representing each wind turbine individually, while the second model is an aggregation, representing the wind farm by a single wind turbine.

A comprehensive set of measured data is applied to support and validate the assumptions and results of the simulation models. Approximately 1 year of measurements of power and wind speeds from the two large offshore wind farms in Denmark (Horns Rev and Nysted) is used. The data are acquired with 1 s sampling rates and with individual measurements on all wind turbines.

Since the wind speed fluctuations are stochastic, a given set of specifications to the simulation models including wind farm layout and meteorological conditions can result in different simulated time series, depending on the initialisation of a random seed. Thus, the simulated wind speed time series and the corresponding power time series are not predictions of an expected sequence. However, the simulated time series should have the

DOI: 10.1002/we

same stochastic properties as the measured time series. In this context, the key stochastic property is the power spectral density (PSD), i.e. the energy of the fluctuations given in the frequency domain.

Model Description

Diversified Model

Figure 1 shows a block diagram of the diversified model with individual representation of a number N of wind turbines. The PSD $S_{u[i]}(f)$ of the wind speed in a fixed point in the hub height of each wind turbine i is given as input. For each wind turbine, a rotor wind block calculates the PSD $S_{u_{eq}[i]}(f)$ of an equivalent wind speed $u_{eq[i]}(t)$, which includes the smoothing of the wind speed due to the weighted averaging over the rotor. The kernel of the model is the time series simulator, which outputs time series $u_{eq[i]}(t)$ of the equivalent wind speeds, taking into account the correlation between the wind speeds expressed in the $N \times N$ coherence functions $\gamma_{[rc]}(f)$. The wind turbine blocks then calculates the produced electrical power $P_{wt[i]}(t)$. Finally, the power of all wind turbines is summed to provide the wind farm output power $p_{wf}(t)$.

The diversified model used in this paper is a further development of the wind models for simulation of power fluctuations from wind farms, described by Sørensen *et al.*[2] The model in Sørensen *et al.*[2] is focused on simulation of the power quality characteristics defined in the International Electrotechnical Commission standard IEC 61400-21.[3] The simulated power quality characteristics are a maximum of 0.2 s power, reactive power and flicker emission from the wind farm. The model is verified for that purpose in Hansen *et al.*[4] The present model focuses on longer term fluctuations as described in the introduction.

The main development of the present model compared to Sørensen *et al.*[2] is on the input side, where the PSD and coherence functions applied in the present paper are changed significantly by including empirical results from Risøs test site for large wind turbines in Høvsøre. So far, only temporary results of the Høvsøre analyses have been published by Sørensen et al.,[5] but in the present paper, updated analysis results for power spectral densities and coherences will be presented and applied.

Another difference is that the rotor wind blocks in Figure 1 are moved to the frequency domain (i.e. before the time simulator box) in the present model, whereas the model described in Sørensen *et al.*[2] applied the time series simulator on $s_{u[i]}(f)$ and therefore had the hub height wind speed $u_{[i]}(t)$ as outputs.

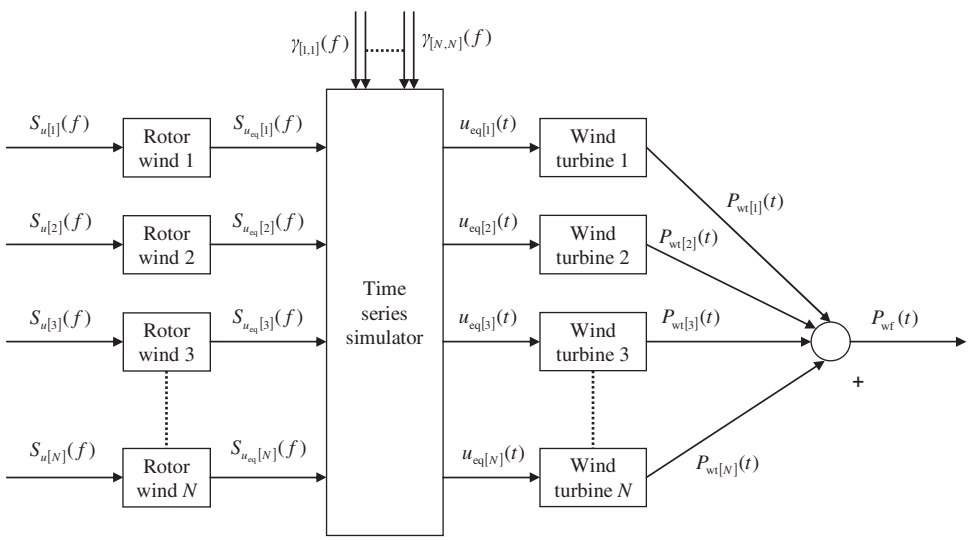

Figure 1. Overall structure of diversified model for simulation of power fluctuations

DOI: 10.1002/we

Finally, the present model simplifies the dynamics because the focus is on fluctuations with 1 min period time or more. Thus, the present model neglects the periodic (3p) components of power fluctuation, which are crucial for simulation of flicker emission, but are much faster than the time scale in focus here. Another simplification is that the present model uses a steady-state representation of the wind turbine, whereas the wind turbine model in Hansen *et al*.[4] included dynamics of the mechanical transmission system as well as the electrical system.

PSD of Wind Speed

Analytical expressions for PSD functions of wind speed in a fixed point can be found in the literature and in standards. Van Karman[6] proposed a PSD for wind speeds in 1948, and Kaimal[7] proposed another type of PSD in 1972. The international standard IEC 61400-1[8] for design requirements to wind turbines specifies a Kaimal type PSD function $S_{\mathrm{IEC}}(f)$, which can be used in wind turbine design. The same PSD is chosen for the present work, and it can be expressed as a double sided spectrum according to

$$S_{\mathrm{IEC}}(f) = \sigma^2 \cdot \frac{2 \cdot \frac{L_1}{V_0}}{\left(1 + 6 \cdot \frac{L_1}{V_0} \cdot f\right)^{5/3}}, L_1 = \begin{cases} 5.67 \cdot z, & z \le 60\,\mathrm{m} \\ 340.2\,\mathrm{m}, & z > 60\,\mathrm{m} \end{cases} \tag{1}$$

V_0 is the average wind speed and σ is the standard deviation (SD) of the wind speed in a 10 min interval; L_1 is the length scale, and z is the height above ground, i.e. the hub height in our case.

Inside a wind farm, IEC 61400-1 recommends to apply the model proposed by Frandsen[9] to include the added turbulence generated by upwind turbines in the structural design of wind turbines. Frandsen proposes to calculate the turbulence $\sigma = \sigma_{\mathrm{wf}}$ according to

$$\sigma_{\mathrm{wf}} = \frac{1}{2}\left(\sqrt{\left(\frac{0.36 \cdot V_0}{1 + 0.2 \cdot \sqrt{S_1 \cdot S_2 / C_{\mathrm{T}}}}\right)^2 + \sigma_{\mathrm{am}}^2} + \sigma_{\mathrm{am}}\right) \tag{2}$$

where σ_{am} is the turbulence in the ambient flow. s_1 and s_2 are the separations between rows and columns, respectively, in the farm, normalised by the wind turbine rotor diameter. C_{T} is the wind turbine thrust coefficient.

For simulation of power fluctuations, $\sigma = \sigma_{\mathrm{am}}$ is chosen to be used for the wind turbines in the front with expected free inflow, and $\sigma = \sigma_{\mathrm{wf}}$ for the remaining wind turbines inside the wind farm.

According to e.g. Courtney and Troen,[10] there is a significant variability of the wind speed at lower frequencies, which is not included in the Kaimal spectrum. The Kaimal-type PSD functions are valid only for shorter time scales, corresponding to what is normally considered in mechanical design of wind turbines, i.e. from 0.02 to 600.0 s. For simulations of wind farm power fluctuations, the PSD functions are required on a longer time scale (up to several hours). The Høvsøre measurements have been applied to fit the PSD $S_{\mathrm{LF}}(f)$ for low frequencies, and the fit is expressed as

$$S_{\mathrm{LF}}(f) = (\alpha_{\mathrm{LF}} \cdot V_0 + \beta_{\mathrm{LF}})^2 \frac{\frac{z}{V_0}}{\left(\frac{z \cdot f}{V_0}\right)^{5/3} \cdot \left(1 + 100 \cdot \frac{z \cdot f}{V_0}\right)} \tag{3}$$

Assuming $\beta_{\mathrm{LF}} = 0$, $\alpha_{\mathrm{LF}} = 0.0046$ has been estimated based on Høvsøre measurements. The input spectra $S_{\mathrm{u[i]}}(\mathrm{f})$ in Figure 1 include high frequencies as well as low frequencies according to

$$S_{u[i]}(f) = S_{\mathrm{Kai}}(f) + S_{\mathrm{LF}}(f) \tag{4}$$

Coherence Function

In equation (1), the empirical coherence functions suggested by Schlez and Infield[11] are used. However, these expressions are mainly based on measurements with 18 m high masts with distances up to 102 m. Based on the

DOI: 10.1002/we

measurements in 80 m height with up to 1.2 km distances in Høvsøre, parameters for the decay factor $A_{[r,c]}$ are fitted to a coherence function $\gamma_{[r,c]}(f)$ between wind turbine number r and wind turbine number c according to

$$\gamma_{[r,c]}(f) = \exp\left(-\left(A_{[r,c]}\frac{d_{[r,c]}}{V_0} + j2\pi\tau_{[r,c]}\right)\cdot f\right) \tag{5}$$

Here, $d_{[r,c]}$ is the distance between wind turbine r to wind turbine c, and $\tau_{[r,c]}$ is the time it takes a wave to travel from wind turbine r to wind turbine c, which depends on the wind speed and the inflow angle $\alpha_{[r,c]}$ of the wind speed to the line between wind turbine r and wind turbine c as defined in Sørensen *et al*.[2] For flow with inflow angles $\alpha_{[r,c]}$ between these points, Schlez and Infield suggest to use the expression

$$A_{[r,c]} = \sqrt{\left(A_{\text{long}}\cos\alpha_{[r,c]}\right)^2 + \left(A_{\text{lat}}\sin\alpha_{[r,c]}\right)^2} \tag{6}$$

A_{long} is the decay factor when the flow is longitudinal, i.e. when the wind direction points directly from wind turbine r to wind turbine c. A_{lat} is the decay factor when the flow is lateral, i.e. when the wind direction is perpendicular to the line between wind turbine r and wind turbine c.

Based on the Høvsøre measurements representing horizontal distances between 300 m and 1200 m, the coherence function has been fitted to the decay factors:

$$A_{\text{long}} = 4 \tag{7}$$

$$A_{\text{lat}} = \frac{V_0}{2m/s} \tag{8}$$

Rotor Wind Model

The idea in the rotor wind model is to generate an equivalent wind speed which can be applied to a simplified aerodynamic model to simulate the aerodynamic torque or power on the wind turbine shaft. The rotor wind block includes the smoothing of the wind speed due to the weighted averaging over the rotor.

Neglecting the periodic components, the rotor block smoothing of the wind turbine can be expressed as a wind turbine admittance function $F_{wt}(f)$ defined as

$$F_{\text{wt}}(f) = \frac{S_{u_{\text{eq}}}(f)}{S_u(f)} \tag{9}$$

Assuming different coherence functions and wind speed weightings in the rotor plane, the admittance function has been solved numerically by Sørensen.[12] IEC 61400-21 specifies the coherence function $\gamma_{\text{IEC}}(f)$ in the rotor plane according to

$$\gamma_{\text{IEC}}(f) = \exp\left(-12\cdot\sqrt{\left(\frac{d\cdot f}{V_0}\right)^2 + \left(0.12\cdot\frac{d}{L_1}\right)^2}\right) \tag{10}$$

Calculating the admittance function numerically with the coherence function in equation (10), this admittance function is fitted to the analytical expression

$$F_{\text{wt}}(f) = \frac{1}{\left(1+\left(\sqrt{f^2+f_1^2}/f_0\right)^{4/3}\right)^{3/2}},\ f_0 = \frac{\sqrt{2}}{A}\cdot\frac{V_0}{R},\ f_1 = 0.12\cdot\frac{V_0}{L_1} \tag{11}$$

Here, R is the radius of the wind turbine rotor disc and A is the coherence decay factor, i.e. $A \cong 12$ using the coherence function $\gamma_{\text{IEC}}(f)$.

Time Series Simulator

The kernel of the model is the time series simulator, which simulates simultaneous time series $u_{\text{eq}[i]}(t)$ of the N wind speeds indexed i, based on the N PSD's $S_{u_{\text{eq}[i]}}(f)$ of the wind speeds and the $N \times N$ coherence functions

DOI: 10.1002/we

$\gamma_{[r,c]}(f)$ between wind speeds indexed r and c. The applied method is in principle the same as used by Veers[13] to simulate the wind speed field in a wind turbine rotor. However, the coherence function (equation (5)) used in the present model is complex as a consequence of the horizontal travel time for wind speed from one wind turbine to another. Therefore, the method is described below, taking into account that the coherences can be complex.

The first step in the time series simulation method is to generate the $N \times N$ cross power spectral density (CPSD) matrix $\mathbf{S}(f)$ with the elements

$$S_{[r,c]}(f) = \gamma_{[r,c]}(f) \cdot \sqrt{S_{u_{\mathrm{eq}}[r]}(f) \cdot S_{u_{\mathrm{eq}}[c]}(f)} \tag{12}$$

In order to ensure that the simulated time series have the correct CPSD matrix $\mathbf{S}(f)$, the Fourier transforms $\mathbf{U}(f)$ of the output time series must fulfill equation (13) for all frequencies f, where $\langle x \rangle$ denotes the ensemble mean value of the stochastic variable x; x^* denotes complex conjugated of x, and $\boldsymbol{x}^{\mathrm{T}}$ is the transposed of vector or matrix $\boldsymbol{x}$. According to e.g. Newland[14], the PSD $S(f)$ of a stochastic time series $u(t)$ can be estimated by splitting $u(t)$ into a number of equidistant segments, calculate the Fourier transform $\mathrm{U}(f)$ of each segment, and finally determine the PSD as expressed in Reference 13.

$$\mathbf{S}(f) \cdot \Delta f = \left\langle \boldsymbol{U}(f) \cdot \boldsymbol{U}^{*\mathrm{T}}(f) \right\rangle \tag{13}$$

Equation (13) has infinity of solutions. To find one of those solutions, the vector $\boldsymbol{U}(f)$ is separated into a deterministic matrix $\mathbf{U}_{\mathrm{LT}}(f)$ and a stochastic vector $\boldsymbol{N}(f)$ according to

$$\boldsymbol{U}(f) = \mathbf{U}_{\mathrm{LT}}(f) \cdot \boldsymbol{N}(f) \tag{14}$$

$\mathbf{U}_{\mathrm{LT}}(f)$ is a lower triangular $N \times N$ matrix, i.e. all elements above the diagonal are zero, and $\boldsymbol{N}(f)$ is an N element vertical vector of unity noise elements, which are uncorrelated stochastic variables, i.e.

$$\left\langle \boldsymbol{N}(f) \cdot \boldsymbol{N}^{*\mathrm{T}}(f) \right\rangle = \mathbf{E} \tag{15}$$

where $\mathbf{E}$ is the unity matrix with ones in the diagonal and zeroes outside the diagonal.

Inserting equation (14) in equation (13) and applying equation (15), each element $S_{[r,c]}(f)$ in $\mathbf{S}(f)$ must fulfill the relation

$$S_{[r,c]}(f) \cdot \Delta f = \sum_{i=1}^{c} U_{\mathrm{LT}[r,i]} \cdot U_{\mathrm{LT}[c,i]}^{*}, \; c \le r \tag{16}$$

Applying equation (16), the elements in $\mathbf{U}_{\mathrm{LT}}(f)$ can be found one by one according to

$$U_{\mathrm{LT}[r,c]} = \begin{cases} \dfrac{S_{[r,c]}(f) \cdot \Delta f - \sum_{i=1}^{c-1} U_{\mathrm{LT}[r,i]} \cdot U_{\mathrm{LT}[c,i]}^{*}}{U_{\mathrm{LT}[c,c]}}, & c < r \\ \sqrt{S_{[r,r]}(f) \cdot \Delta f - \sum_{i=1}^{r-1} \left| U_{\mathrm{LT}[r,i]} \right|^2}, & c = r \end{cases} \tag{17}$$

To summarise the sequence of the time series simulator: for each frequency, first, the CPSD matrix $\mathbf{S}(f)$ is calculated according to equation (12), then $\mathbf{U}_{\mathrm{LT}}(f)$ is calculated using equation (17), then a random function is applied to get $\boldsymbol{N}(f)$ as a two-dimensional (with uncorrelated real and imaginary parts) Gaussian distribution fulfilling equation (15), and finally $\boldsymbol{U}(f)$ is calculated according to equation (14). When this has been done for all frequencies, the output time series are found as the inverse Fourier transform of $\boldsymbol{U}(f)$.

Wind Turbine Model

Finally, the wind turbine blocks in Figure 1 are needed to model the conversion of wind fluctuations to power fluctuations. For the present purpose, a steady-state model of the wind turbine is applied, based on the power curve of the wind turbine. A more advanced approach including the dynamics of rotor speed and generator power control could be applied if higher frequencies of power fluctuations are in focus. This issue is discussed further in the analysis part of the paper.

DOI: 10.1002/we

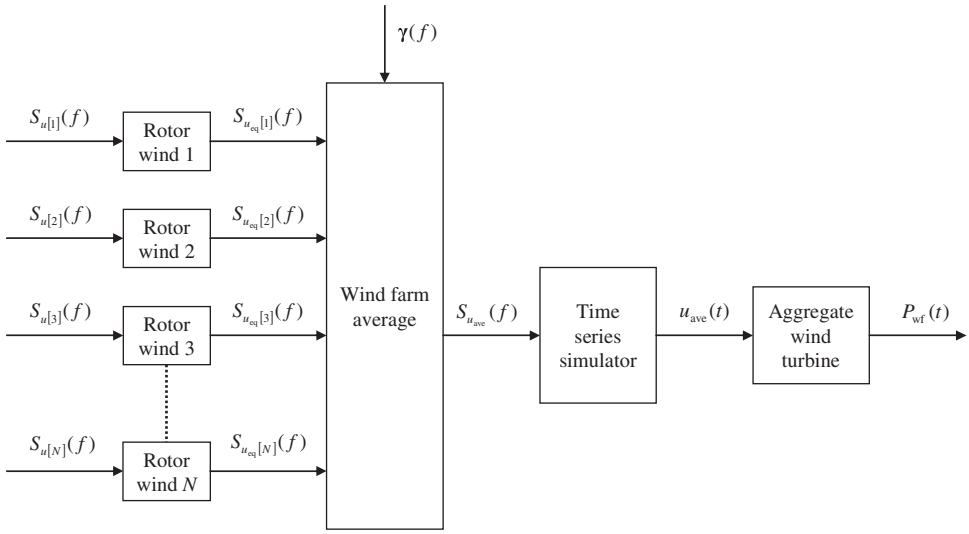

Figure 2. Overall structure of aggregated model for simulation of power fluctuations

Aggregated Model

The simulation times of the diversified model in Figure 1 increases almost with the square of the number of wind turbines. The main reason for this is the required calculation time of equation (17) in the time series simulation. Besides, if the power fluctuation model would be applied in a model to simulate the power and frequency control in a power system, the wind turbines would not be represented individually, but rather by a single or a few aggregated wind turbines. Therefore, an aggregation of the diversified model is suggested.

A simple aggregation is illustrated in Figure 2. For simplicity, the present aggregation is based on the assumption that the rated power of all wind turbines is the same. If this is not the case, the averaging can be replaced by a weighted average. Moreover, the aggregation assumes that the wind turbines are linear, which is a rough approximation when the wind speed is close to rated. Still, this aggregation is a reasonable compromise between accuracy and simulation time.

Wind Farm Average Wind Speed

The wind farm average block in Figure 2 calculates the PSD function of the average of N wind speeds, based on the PSD functions of the N wind speeds and the coherence functions between them. In the time domain, the relation is simply

$$U_{\text{ave}}(t) = \frac{1}{N}\sum_{i=1}^{N} u_{\text{eq}[i]}(t) \tag{18}$$

In the frequency domain, the corresponding relation between the PSD functions is

$$S_{u_{\text{ave}}}(f) = \frac{1}{N^2}\sum_{r=1}^{N}\sum_{c=1}^{N} S_{[r,c]}(f) \tag{19}$$

$S_{[r,c]}(f)$ are the elements in the CPSD matrix $\mathbf{S}(f)$. Inserting equation (12) in equation (19), and assuming that the PSDs of the wind speeds are the same at all wind turbines, i.e. $S_{u_{\text{eq}[r]}}(f) = S_{u_{\text{eq}[c]}}(f) = S_{u_{\text{eq}}}(f)$ yields

$$S_{u_{\text{ave}}}(f) = \frac{S_{u_{\text{eq}}}(f)}{N^2}\sum_{r=1}^{N}\sum_{c=1}^{N} \gamma_{[r,c]}(f) \tag{20}$$

DOI: 10.1002/we

With these assumptions, a wind farm admittance function $F_{wf}(f)$ is defined to characterise the smoothing effect of the wind farm according to

$$F_{\mathrm{wf}}(f) = \frac{S_{u_{\mathrm{ave}}}(f)}{S_{u_{\mathrm{eq}}}(f)} = \frac{1}{N^2}\sum_{r=1}^{N}\sum_{c=1}^{N}\gamma_{[r,c]}(f) \tag{21}$$

Aggregated Wind Turbine

To mitigate the error due to the non-linear power curve, Nørgaard and Holttinen[15] proposed an aggregated power curve to represent multiple wind turbines, where the sharp curves of the single wind turbine power curve (i.e. the strong non-linearities) are partly smoothed.

The aggregated power curve proposed by Nørgaard and Holttinen was intended for electricity market modelling, applying large time scales (1 h average values) and geographic areas (200–500 km regions). In the wind farm cases studied in the present paper, the distances are much smaller, and therefore using 1 h averages, the difference between aggregated and single wind turbine power curves should be less than in Nørgaard and Holttinen.[15] But in the present case, the averaging time used is only 1 min, and therefore it could still be relevant to replace the single turbine power curve with an aggregated power curve.

Wind Farm Sites and Data Acquisition

Horns Rev

Horns Rev wind farm is the first large wind farm connected directly to the transmission system in Denmark. It consists of 80 Vestas V80 variable speed wind turbines. The rated power of the V80 turbines is 2 MW, and the rotor diameter is 80 m.

Figure 3 shows the layout of Horns Rev wind farm. The distance between the turbines is 560 m in the rows as well as columns, corresponding to seven rotor diameters.

The measured data are acquired by the Supervisory Control and Data Acquisition (SCADA) system used by the wind farm main controller, which off course has the first priority. The acquired data originate from the wind turbine control systems. The wind speed is measured on the nacelle of each wind turbine with ultrasonic sensors. The power is measured by the control system on the low-voltage terminals as a sum of rotor and stator powers. Finally, the yaw position registered in the wind turbine is used to indicate the wind direction. Wind speed, power and yaw position are logged with 1 Hz sampling frequency.

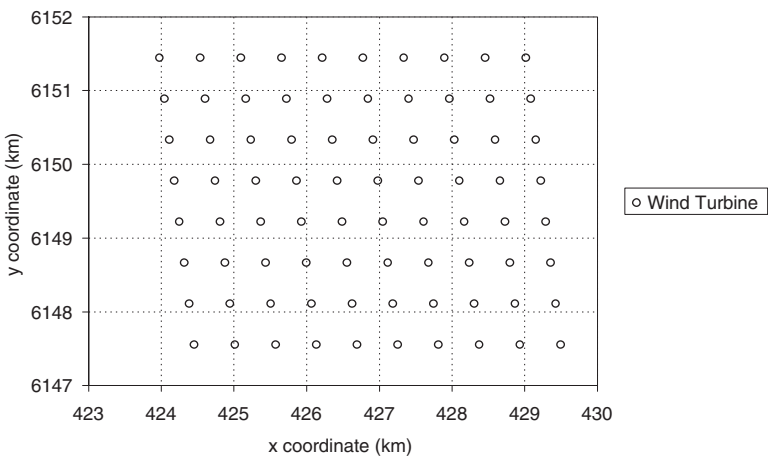

Figure 3. Horns Rev wind farm

DOI: 10.1002/we

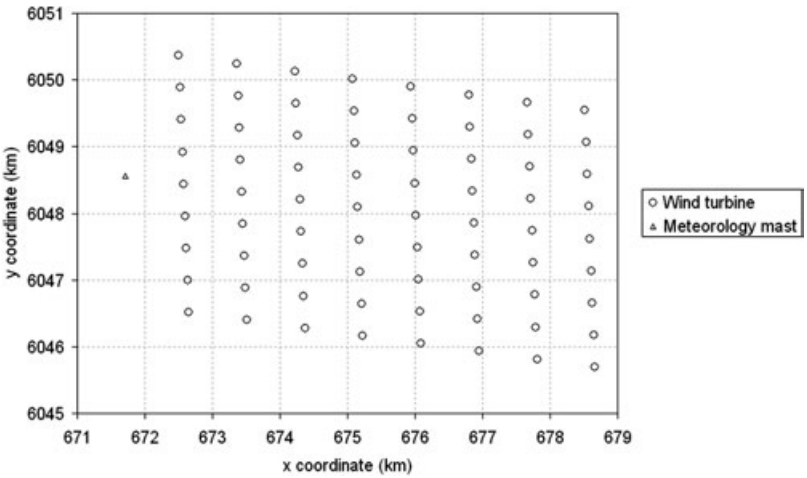

Figure 4. Nysted wind farm

Nysted

Nysted wind farm is the second large wind farm connected directly to the transmission system in Denmark. It is connected to the East Danish power system. It consists of 72 Siemens SWT-2.3-82 fixed speed wind turbines. The rated power of the SWT-2.3-82 turbines is 2.3 MW, and the rotor diameter is 82 m.

Figure 4 shows the layout of Nysted wind farm. The distance between the turbines in a column is 481 m corresponding to 5.9 rotor diameters, while the distance between the turbines in a row is 867 m corresponding to 10.6 rotor diameters.

Like in Horns Rev, the measured data are acquired by the SCADA system used by the wind farm main controller with 1 Hz sampling frequency. The acquired data originate from the wind turbine control systems and from a meteorology mast indicated in Figure 4. The measurements from the wind turbine control systems are the wind speed measured on the nacelle of each wind turbine with cup anemometer, the power measured by the control system on the low-voltage terminals and the yaw position. The meteorology mast provides wind speed and wind direction measurements in hub height.

Analyses

The analyses presented in this chapter are based on measurements from both wind farms. The measurements are divided into 2 h segments according to the time range in focus for the large power fluctuations.

Power Spectral Densities

The purpose of this section is to assess the specified PSDs for fixed-point wind speeds in the model chapter by comparing the models to measurements. In principle, the specified PSDs correspond to what the wind speed would be if the wind turbine is not there. Thus, when applying measurements on the nacelle, a complete match should not be expected.

Figure 5 shows PSDs in Nysted measured on the meteorology mast and on the nacelles of wind turbines in the west-most column A. Only segments with wind directions between south-west and north-west, and with mean wind speeds between 8 and 9 $\mathrm{m\,s^{-1}}$ are included. These measured PSDs are compared to the model PSD according to equations (4), (3) and (1), using the ambient turbulence intensity in equation (1), which is measured to 6.3% on the mast for the selected time series.

The differences in fluctuations in the low frequencies $f < 0.01$ Hz are the most important for this study, because it is in the time range of main interest for the power fluctuations. The curves indicate that the

DOI: 10.1002/we

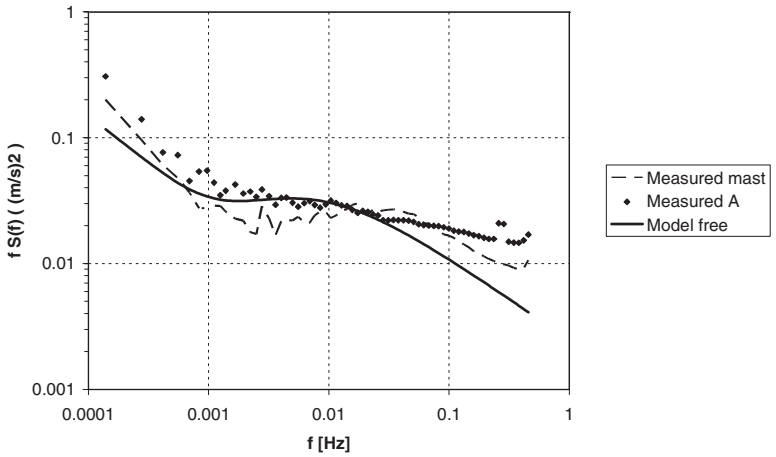

Figure 5. PSDs for mean wind speeds between 8 and 9 m s^{-1} with western wind measured in Nysted offshore wind farms

measured fluctuations at very low frequencies $f < 0.001$ Hz are a little higher than what is obtained by the Høvsøre low frequency fit in equation (3). A possible explanation for that difference could be the different climate in the Baltic Sea where Nysted wind farm is located and Høvsøre test site with wind from the North Sea. But conclusions should not be drawn on the limited data.

Another difference is in the distribution of fluctuation for frequencies $f > 0.001$ Hz. The measurements in the meteorology mast should be very close to the model, because the model covers undisturbed flow. The 10 min SD is the same in mast measurements and the model, but parameter studies have shown that the model could be fitted very close to the measurements if a two to three times lower length scale L_1 is selected in equation (1).

Finally, it is seen that there is a significant difference between the nacelle measurements in column A and the mast measurements. Generally, there are more fluctuations on the nacelle wind speeds, which is as expected, because local turbulence is generated by the wind turbine rotor and nacelle. The increase is strongest for high frequencies $f > 0.1$ Hz. This frequency range is very sensitive to aliasing of fluctuations at frequencies $f > 0.5$ Hz, because the PSDs are low. There is also an increased power fluctuation on the nacelle in the frequency interval $0.001\,\text{Hz} < f < 0.01\,\text{Hz}$, which is more surprising. However, the differences are not expected to be critical to the simulation performance.

The PSDs measured on wind turbines in column A in Nysted and the corresponding model for free turbulence are shown again in Figure 6, this time with measured PSD in column E inside the wind farm and the corresponding model using the SD $\sigma = \sigma_{\text{wf}}$ according to equation (2) in equation (1).

The corresponding PSDs are shown for Horns Rev in Figure 7. The same western wind direction and wind speed interval between 8 and 9 m s^{-1} is selected. The ambient turbulence intensity is estimated to 6.5% based on the measurements in column A.

Figure 7 shows a significant increase in the measured PSDs for frequencies $f > 0.07$ Hz, which is due to aliasing. The reason why the aliasing is much more visible in Horns Rev than in Nysted is that the wind speeds are measured with ultrasonic sensors in Horns Rev and with cup anemometers in Nysted. The cup anemometers are filtering the fluctuations significantly before they are sampled, and therefore there is very little energy above 0.5 Hz to be aliased. Unlike that, the ultrasonic sensor captures the significant high-frequency wind variations on the nacelle.

Rotor Wind

The rotor wind blocks in Figure 1 cannot be verified directly with the available measurements, because the equivalent wind speeds $u_{\text{eq}[i]}(t)$ are not measured. Measurement of the equivalent wind speed would require

DOI: 10.1002/we

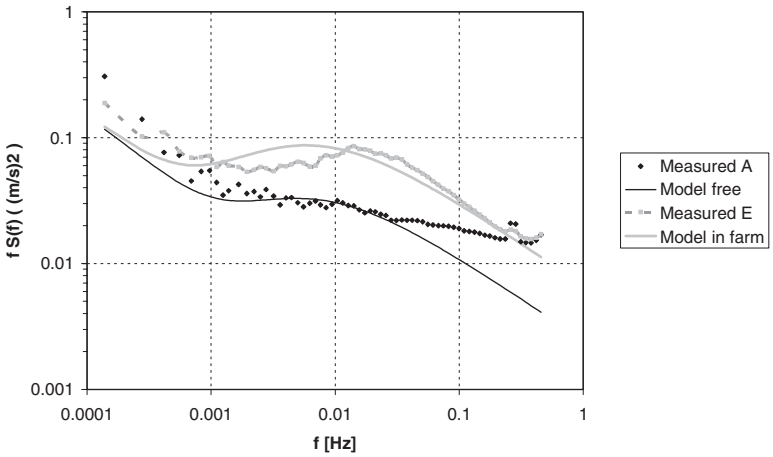

Figure 6. Average PSDs for Nysted turbines in the columns A (free) and E (inside wind farm) compared to model for free turbines and turbines inside wind farm. Wind direction between south-west and north-west. 8–9 m s^{-1} average wind speed

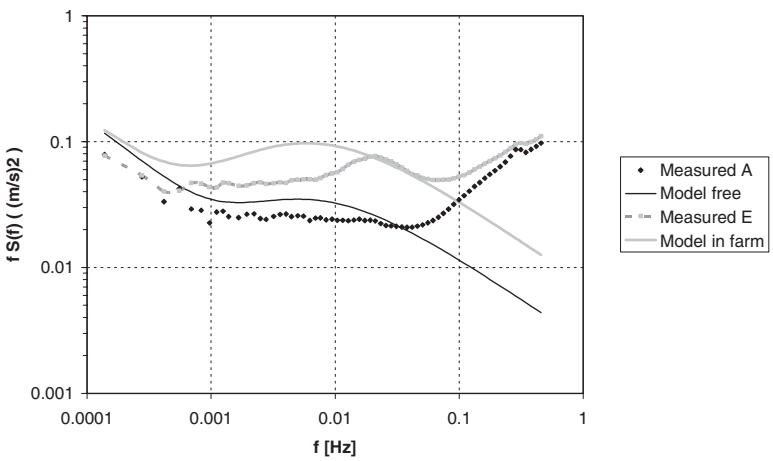

Figure 7. Average PSDs for Horns Rev turbines in the columns A (free) and E (inside wind farm) compared to model for free turbines and turbines inside wind farm. Wind direction between south-west and north-west. 8–9 m s^{-1} average wind speed

wind speed measurements distributed over the whole rotor. However, the power measurements and the power curve can be applied to estimate the equivalent wind speeds when the power is below rated, assuming that the wind turbine dynamics between wind speed and power can be neglected.

This is done for the Siemens wind turbines in Nysted in Figure 8. Only 2 h segments with the average wind speed between 8 and 9 m s^{-1} are included. The wind turbine admittance function is then estimated, calculating it according to the PSD ratio definition in equation (9). The rotor wind model is calculated according to equation (11).

For the important frequencies $f < 0.01$ Hz, it is seen that the model slightly overestimates the admittance, which would result in a corresponding overestimation of the power fluctuations in that frequency range. For higher frequencies, the estimate is greater than the model. There is a distinct, very narrow 1p originating from the power fluctuations. Such a narrow 1p can be explained by a small pitch angle unbalance, which is difficult

DOI: 10.1002/we

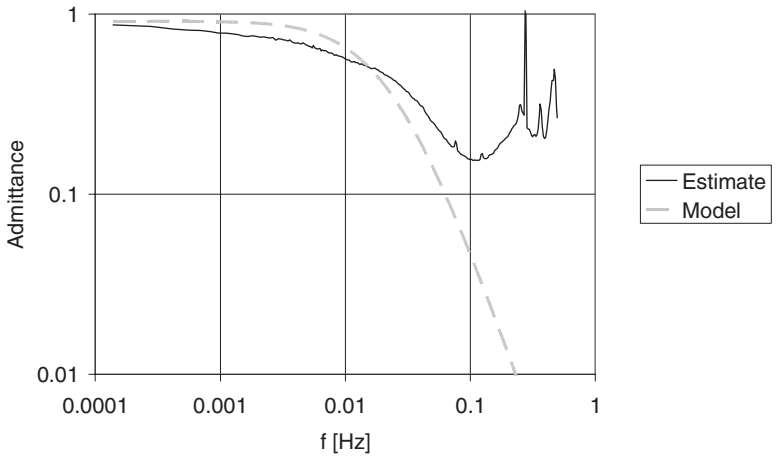

Figure 8. Estimated wind turbine admittance function for the Siemens wind turbine in Nysted compared to equation (11). The average wind speed is in the interval 8–9 m s^{-1}

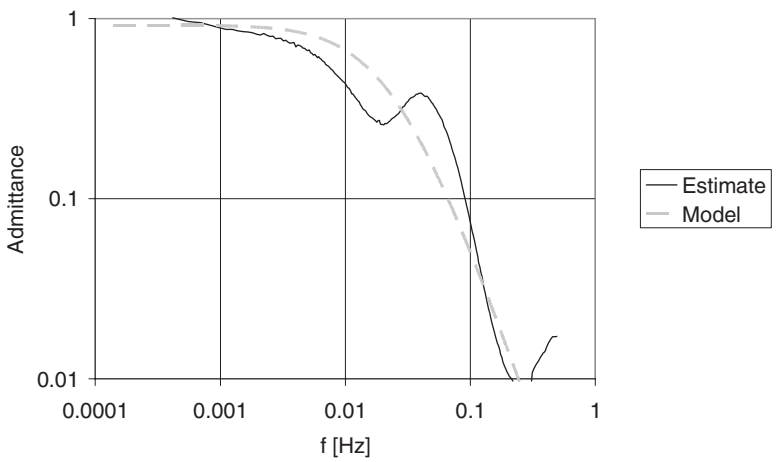

Figure 9. Estimated wind turbine admittance function for the Vestas wind turbine in Horns Rev compared to equation (11). The average wind speed is in the interval 8–9 m s^{-1}

to avoid. The remaining difference for higher frequencies is a combination of low eigenfrequencies (tower modes) and aliasing of variations above 0.5 Hz. Thus, the model can be used for frequencies $f < 0.02$ Hz, corresponding to period times higher than 50 s.

The same estimation and model calculation is shown on the Vestas V80 wind turbine in Horns Rev in Figure 9. The spectra $S_u(f)$ of the nacelle wind speed measurements have been corrected to compensate for the aliasing observed in Figure 5. For low frequencies, the overestimation of the admittance function looks even more significant in this case. For higher frequencies, the estimated admittance has a local maximum around 0.04 Hz. These observations are probably influenced by the variable speed control of the wind turbine, but also in this case, it can be concluded that the model is conservative and acceptable for frequencies $f < 0.02$ Hz.

Wind Turbines

The relation between the single turbine power curve and the aggregated power curve has been investigated applying the measured data for Horns Rev to produce these two power curves. The result is shown in Figure 10.

DOI: 10.1002/we

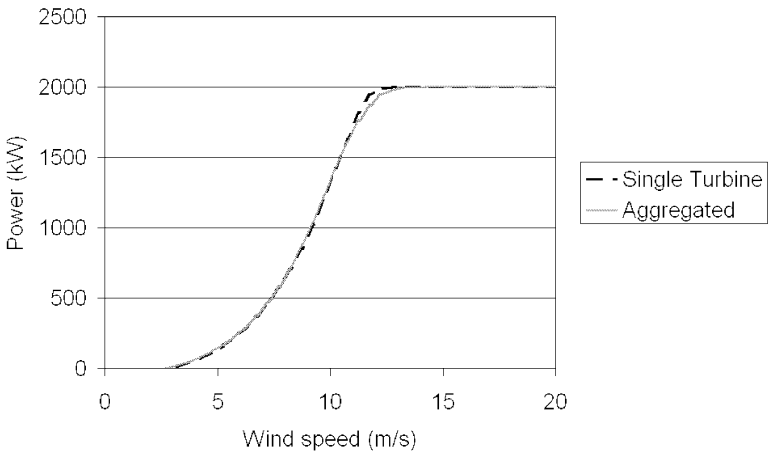

Figure 10. Average of single turbine power curves and aggregated power curve based on 1 min averages of wind speed and power

It should be noted that the power curves in Figure 10 are not measured according to standards. For instance, the wind speeds are measured on the nacelle, and no correction for air pressure has been applied. However, the relative difference between the single turbine and aggregated power curves is very reliable.

The single turbine power curve is calculated as the average of power curves for all wind turbines, i.e. the average of the relation between $u_{[i]}(t)$ and $P_{\mathrm{wt}[i]}(t)$. The aggregated power curve is determined by the average of wind speeds and average of produced power for the online wind turbines.

The conclusion is that the single turbine power curve can be applied, but it is better to use the aggregated power curve. This can be more important for larger wind farms.

Park Scale Average Wind

The wind farm smoothing is characterised by the wind farm admittance function $F_{\mathrm{wf}}(f)$ in equation (22). Since the equivalent wind speed $u_{\mathrm{eq}[i]}(t)$ is not measured, the wind farm admittance function is estimated based on the nacelle wind speed $u_{[i]}(t)$ instead, and the corresponding average wind speed $u_{\mathrm{ave}}(t)$ is the average of the nacelle wind speeds measured on all wind turbines.

Figure 11 shows the estimated admittance function using measurements in Horns Rev with western wind direction and wind speeds from 8 to 9 $\mathrm{m\,s^{-1}}$. The estimated admittance function is compared to corresponding admittance functions of simulated wind speeds, using the coherence decay factors proposed by Schlez and Infield[10] and the Høvsøre decay factors.

The result indicates that the Schlez decay factors are not realistic for the large distances in the offshore wind farm as it has also been concluded on the Høvsøre studies. The Høvsøre coherence gives good results for frequencies below 0.001 Hz, but for higher frequencies, it overestimates the smoothing effect.

To improve the simulations at higher frequencies, it would be necessary to include a frequency dependency in the coherence decay factors.

Conclusion

There is an increased focus on power fluctuations from large offshore wind farms and the impact that this has on the power and frequency control in the power systems. Modelling of these power fluctuations will enable system operators to simulate the expected power fluctuations with a specified wind power development scenario. This is useful to calculate the need for reserves to balance the power fluctuations.

DOI: 10.1002/we

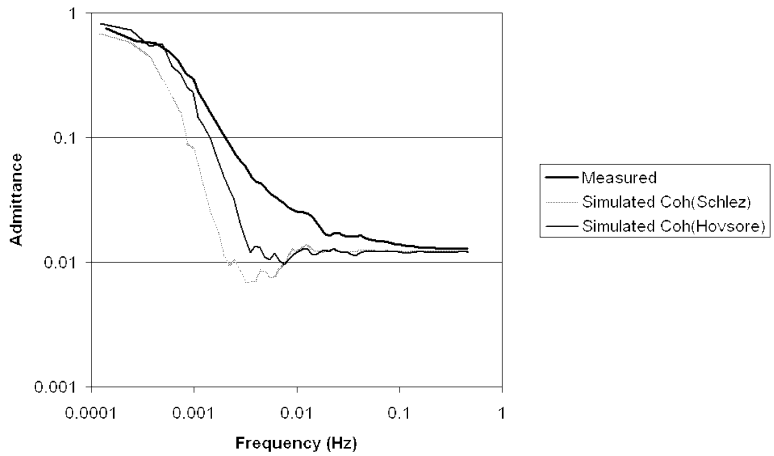

Figure 11. Admittance functions for smoothing effect of wind farm, calculated for measured data and for simulations with Schlez and Høvsøre coherences (Cohs), respectively

This paper has presented a diversified model representing each wind turbine individually and an aggregated model lumping the wind turbines. Aggregation is necessary to support system studies.

The developed power fluctuation models focus on the time range between minutes and a few hours, corresponding to frequencies in the interval from 0.0001 to 0.01 Hz. Fluctuations at higher frequencies are assumed to be filtered effectively for large wind farms, and this has been confirmed by the analysis of the park scale average wind.

The PSDs proposed in the model agree reasonable well with the measured PSDs in Horns Rev and Nysted. The main deviation is at high frequencies and can be explained by aliasing, i.e. due to sampling of instantaneous values which are not filtered before they are sampled. However, since focus is on the lower frequencies which contribute most to the wind farm power fluctuations, the comparison with measurements shows that the applied PSD is acceptable for the purpose of simulating power fluctuations.

The wind farm smoothing seems to fit quite well in the frequency interval from 0.0001 to 0.001 Hz. There is a significant difference from measurements on the wind farm smoothing in the interval between 0.001 and 0.01 Hz. An improvement of the models in that frequency interval will require a deeper study of the coherence in the interval.

Acknowledgements

The work presented in this paper is done in the research project Power Fluctuations from Large Offshore Wind Farms financed by the Danish Transmission System Operator Energinet.dk as PSO 2004 project number 6506. A. Vigueras-Rodríguez gets financial support from the Spanish Ministerio de Educación y Ciencia through the programme Becas FPU.

References

1. Akhmatov V, Kjaergaard JP, Abildgaard H. Announcement of the large offshore wind farm Horns Rev B and experience from prior projects in Denmark. *European Wind Energy Conference, EWEC 2004*, London, 2004.
2. Sørensen P, Hansen AD, Rosas PAC. Wind models for simulation of power fluctuations from wind farms. *Journal of Wind Engineering and Industrial Aerodynamics.* 2002; 90: 1381–1402.
3. IEC 61400-21. *Wind Turbine Generator Systems. Part 21. Measurement and Assessment of Power Quality Characteristics of Grid Connected Wind Turbines*. International Electrotechnical Commision, Geneva, 2001.

DOI: 10.1002/we

4. Hansen AD, Sørensen P, Janosi L, Bech J. Wind farm modelling for power quality. *Proceedings of IECON 2001*, Denver, Colorado, USA, September 2001.
5. Sørensen P, Mann J, Paulsen US, Vesth A. Wind farm power fluctuations. *Euromech 2005*, Kassel, 2005.
6. von Karman T. Progress in the statistical theory of turbulence. *Proceedings of the National Academy of Sciences of the United States of America.* 1948; **34**: 530–539.
7. Kaimal JC, Wyngaard JC, Izumi Y, Cote OR. Spectral characteristics of surface-layer turbulence. *Quarterly Journal of the Royal Meteorological Society* 1972; **98**: 563–598.
8. IEC 61400-1. *Wind Turbines—Part 1. Design Requirements* (3rd edn). International Electrotechnical Commission, Geneva, 2005.
9. Frandsen S. *Turbulence and Turbulence-Generated Structural Loading in Wind Turbine Clusters*. *Risø-R-1188(EN)*, Risø National Laboratory, Roskilde, 2007. Available online: http://www.risoe.dk/rispubl/VEA/reapdf/ris-r-1188.pdf
10. Courtney M, Troen I. Wind speed spectrum from one year of continuous 8 Hz measurements. *Proceedings of 9. Symposium on turbulence and diffusion,* Jensen NO, Kristensen L, Larsen SE (eds), Roskilde 30 April–3 May 1990. American Meteorological Society, Boston, MA, 1990, 301–304.
11. Schlez W, Infield D. Horizontal, two point coherence for separations greater than the measurement height. *Boundary-Layer Meteorology* 1998; **87**: 459–480.
12. Sørensen P. *Frequency Domain Modelling of Wind Turbine Structures*. Risø-R-749. Risø National Laboratory, Roskilde 1994.
13. Veers PS. *Three-dimensional Wind Simulation*. SAND88-0152. Sandia National Laboratories: Albuquerque, 1988.
14. Newland DE. An introduction to random vibrations and spectral analysis, 2nd edn, Longman Inc. New York 1984.
15. Nørgaard P, Holttinen H. A multi-turbine power curve approach. *Nordic Wind Power Conference, NWPC 2004*. Gothenburg, 2004.

DOI: 10.1002/we